Scientific Research Publishing

Energy and Power Engineering, 2024, 16, 179-195
https://www.scirp.org/journal/epe
ISSN Online: 1947-3818
ISSN Print: 1949-243X

Numerical Study and Optimization of CZTS-Based Thin-Film Solar Cell Structure with Different Novel Buffer-Layer Materials Using SCAPS-1D Software

Md. Zamil Sultan*, Arman Shahriar, Rony Tota, Md. Nuralam Howlader, Hasibul Haque Rodro, Mahfuja Jannat Akhy, Md. Abir Al Rashik

Department of Electrical and Electronic Engineering, Hajee Mohammad Danesh Science and Technology University, Dinajpur, Bangladesh
Email: *mdzamilsultan@hstu.ac.bd

How to cite this paper: Sultan, M.Z., Shahriar, A., Tota, R., Howlader, M.N., Rodro, H.H., Akhy, M.J. and Rashik, M.A.A. (2024) Numerical Study and Optimization of CZTS-Based Thin-Film Solar Cell Structure with Different Novel Buffer-Layer Materials Using SCAPS-1D Software. *Energy and Power Engineering*, **16**, 179-195.
https://doi.org/10.4236/epe.2024.164009

Received: February 27, 2024
Accepted: April 15, 2024
Published: April 18, 2024

Abstract

This study explored the performances of CZTS-based thin-film solar cell with three novel buffer layer materials ZnS, CdS, and CdZnS, as well as with variation in thickness of buffer and absorber-layer, doping concentrations of absorber-layer material and operating temperature. Our aims focused to identify the most optimal thin-film solar cell structure that offers high efficiency and lower toxicity which are desirable for sustainable and eco-friendly energy sources globally. SCAPS-1D, widely used software for modeling and simulating solar cells, has been used and solar cell fundamental performance parameters such as open-circuited voltage (V_{oc}), short-circuited current density (J_{sc}), fill-factor(FF) and efficiency(η) have been optimized in this study. Based on our simulation results, it was found that CZTS solar cell with $Cd_{0.4}Zn_{0.6}S$ as buffer-layer offers the most optimal combination of high efficiency and lower toxicity in comparison to other structure investigated in our study. Although the efficiency of $Cd_{0.4}Zn_{0.6}S$, ZnS and CdS are comparable, $Cd_{0.4}Zn_{0.6}S$ is preferable to use as buffer-layer for its non-toxic property. In addition, evaluation of performance as a function of buffer-layer thickness for $Cd_{0.4}Zn_{0.6}S$, ZnS and CdS showed that optimum buffer-layer thickness for $Cd_{0.4}Zn_{0.6}S$ was in the range from 50 to 150nm while ZnS offered only 50 – 75 nm. Furthermore, the temperature dependence performance parameters evaluation revealed that it is better to operate solar cell at temperature $290K$ for stable operation with optimum performances. This study would provide valuable insights into design and optimization of nanotechnology-based solar energy technology for minimizing global energy crisis and developing

eco-friendly energy sources sustainable and simultaneously.

Keywords

Thin-Film Solar Cell, CZTS, Buffer-Layer, Renewable Energy, Green-House Gases, Efficiency

1. Introduction

Recent year, the greenhouse gases (GHGs) such as carbon dioxide (CO_2), methane (CH_4), nitrous oxide (N_2O) etc. upsurge uninterruptedly in the atmosphere by energy burning and industrial revolution, which is a global warning to everyone in terms of climate change [1]. On the other hand, the reserve of fossil fuels, such as coal, natural gas and oil are limited but the global energy demand increases drastically, therefore continuous fulfilling the global energy demands is a serious issue of concern. Alternately, it is great demand to upsurge potential usage of renewable energy sources for keeping green-clean world as well as for satisfying global high energy requirement simultaneously and sustainably [2] [3] [4]. Renewable solar energy could a vibrant source in this circumstance for energy production by using photovoltaic technology [5] [6], such as solar cell as it is environmentally eco-friendly as well as has enormous globally. However, the relative higher cost [7], flexibility and efficiency limitations of solar cells till remain the biggest problems compared to conventional systems. The problems are expected to be overcome as the technology progresses. For single junction photovoltaic cells, the maximum efficiency is limited to be 33.7% according to the Shockley-Queisser (S-Q) calculations [8]. An approach of using multi-junction solar cells has been considered to overcome the limitation of single junction solar cell [9], however the structure suffers structural complexity. A more humble solution is a thin-film solar cell in terms of cost/watt ratio [10], light weight [11] and flexible fabrication process [12]. Since the fundamental performance parameters of thin-film photovoltaic cells, such as open circuit voltage (V_{oc}), short circuit current density (J_{sc}), fill-factor (FF) and efficiency (η)can be precisely controlled by fabrication materials as well as structures, there is a major scope of research on this device for obtaining better performances by optimizing thin-film structure, structural parameters and their fabrication materials. Therefore, the aims of this study have focused to improve device performance through evaluating absorber layer thickness, buffer layer thickness, buffer layer materials and working temperature. To obtain this, CZTS based thin-film solar cell structure has been studied with three novel buffer layer materials $Cd_{0.4}Zn_{0.6}S$, ZnS and CdS.

Over the recent years, the technologies and significant efficiency improvement of $CuInGaSe_2$ (CIGS) thin-film solar cells have been demonstrated in several reports [13] [14]. However, the scarcity and high prices of In, Ga, and the toxicity of In, Cd, and Se eventually could limit the production growth of this type of so-

lar cells. Cu_2ZnSnS_4 (CZTS) has been considered as a potential alternative compound which contains more abundant elements preferable for the realization of low-cost solar cells. Nevertheless, CZTS is a direct band gap material with high absorption coefficient [15] in order of 10^4 cm^{-1} and contains less toxic material S which is desirable for environment-friendly high performances optoelectronics applications. Several researchers have given a lot of successful work on this CZTS till now [16] [17] [18] [19].

Though CZTS has emerged as a viable solar cell technology, buffer layer tuning remains a challenge. The buffer layer aligns the bands between the CZTS and the window layer while also reducing flaws and interfacial strain caused by the window layer [20]. Among different buffer layer materials, cadmium sulfide (CdS) [21] [22], zinc sulfide (ZnS) [23] [24] and ternary alloy cadmium zinc sulfide (CdZnS) [25] [26] [27] have been attracted more attention to the researchers because of their unique optical and electrical properties suitable for thin-film solar cell structure. CdS has a bandgap of 2.42 eV so that absorbs photons with wavelengths less than 590 nm, therefore covering 24% of the solar spectrum. An environment-friendly material zinc sulfide (ZnS) can also be used as an alternative buffer layer [23]. ZnS has a higher bandgap of 3.5 eV compared to CdS which results in less absorption of low-wavelength photons. It also produces a better interface with CZTS creating a potential barrier to separate the electron-hole pair. The third buffer materials used in this study, $Cd_{0.4}Zn_{0.6}S$ [28] is a ternary compound semiconductor alloy in which band gap energy is 2.98 eV which is suitable for maximum solar energy conversion.

Although, CdS, ZnS and CdZnS have promising performance as buffer layer materials for the thin-film solar cells; as far we know no research work has been reported previously on the comparison among these three novel buffer layer materials for the CZTS-based solar cells. For the first time, this research work explored the best buffer material among these three novel CdS, ZnS and CdZnS materials while CZTS being used as absorber layer. Then, the device structural parameters have also been suggested for the high performance photo-voltaic conversion.

Thus, the main objective of this work is to offer a CZTS solar cell with high efficiency by optimizing devices structure with a suitable buffer layer material. To obtain this, CZTS solar cell device models were numerically simulated and analyzed using SCAPS-1D for various thickness of buffer layer and absorber layer, doping concentrations of absorber layer material and operating temperature as well as for three different buffer layers such as CdS, ZnS, and $Cd_{0.4}Zn_{0.6}S$. Four fundamental solar cell performance parameters, V_{oc}, J_{sc}, FF and η were observed and optimized.

The paper consists of four sections. Section 1 starts the paper with brief introduction of the research paper. In section 2 of this paper, methods and methodology such as proposed structure of thin-films solar cell and simulation method will be discussed. Section 3 represents analysis and optimization of V_{oc}, J_{sc}, FF and η for various thickness of absorber layer and buffer layer, dop-

ing concentration of absorber layer as well as operating temperature for three buffer layer materials CdS, ZnS, and $Cd_{0.4}Zn_{0.6}S$. Section 4 will summarize the results with brief conclusion.

2. Methodology

The schematic diagram of the proposed thin-film solar cell structure, n-ITO/i-ZnO/n-CdS or ZnS or $Cd_{0.4}Zn_{0.6}S$/p-CZTS/p-$MoSe_2$ has been illustrated in Figure 1. In this study, we consider five layered structure. The topmost layer n-type indium tin oxide (ITO) is an electron transport layer (ETL). Intrinsic ZnO is used for carrier multiplication. The n-type buffer layer and p-type CZTS absorber layer formed a pn-junction and a depletion region has been formed at that junction. Finally, the bottom most highly doped p-type $MoSe_2$ is used as hole transport layer (HTL). The solar cell is illuminated under 100 mW/cm^2 with global air mass AM1.5 G solar spectrum at operating temperature 300 K. We have considered ideal conditions for the series (R_s) and shunt (R_{sh}) resistances for the solar cell structure. The simulation of the proposed structure and investigation of the performance parameters have been done by one of the very popular and more reliable computer simulation tools titled, "Solar Cell Capacitance Simulator's one-dimensional simulation software (SCAPS-1D)" invented by Burgelman et al at the Department of Electronics and Information Systems, University of Gent, Belgium [29]. The SCAPS-1D provides the opportunity for solar cell researchers to analyze the device structure effectively [30] [31]. It is a very useful tool used to perform electrical characterizations and spectral responses of solar cells. The parameters of thin film solar cells applied to compute our numerical simulations are listed in Table 1 according to the previous studied research works.

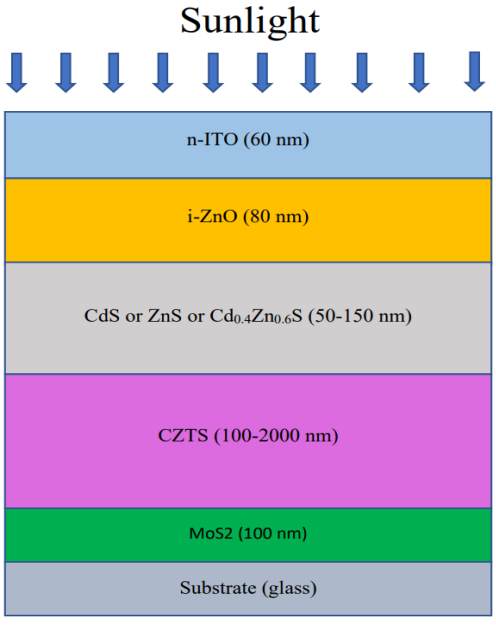

Figure 1. Schematic diagram of proposed thin-film solar cell structure, n-ITO/i-ZnO/n-CdS or ZnS or $Cd_{0.4}Zn_{0.6}S$/p-CZTS/p-$MoSe_2$.

Table 1. Numerical values of different parameters used in this study collected from previous reports [24] [28] [32].

Parameters	MoS_2	CZTS	CdS	ZnS	$Cd_{0.4}Zn_{0.6}S$	i-ZnO	n-ITO
Thickness (nm)	100	100 - 2000	50 - 150	50 - 150	50 - 150	80	60
Bandgap (eV)	1.7	1.5	2.4	3.5	2.98	3.3	3.6
Electron affinity (eV)	4.2	4.5	4.5	4.5	4.2	4.6	4.1
Dielectric permittivity	13.6	10	10	10	9.4	9	10
CB effective density of states (cm^{-3})	2.2×10^{18}	2.2×10^{18}	2.2×10^{18}	1.8×10^{18}	2.2×10^{18}	2.2×10^{18}	2.2×10^{18}
VB effective density of states (cm^{-3})	1.8×10^{19}	1.8×10^{19}	1.8×10^{19}	1.8×10^{19}	1.8×10^{19}	1.8×10^{19}	1.8×10^{19}
Electron thermal velocity (cm s^{-1})	1×10^{7}	1×10^{7}	1×10^{7}	1×10^{7}	1×10^{7}	1×10^{7}	1×10^{7}
Hole thermal velocity (cm^{-1})	1×10^{7}	1×10^{7}	1×10^{7}	1×10^{7}	1×10^{7}	1×10^{7}	1×10^{7}
Electron mobility (cm^2/VJ)	100	100	100	100	270	100	50
Hole mobility (cm^2/V_s)	25	25	25	25	27	25	75
Shallow uniform donor density, N_D (cm^{-3})	0	1×10^{1}	1×10^{18}	5×10^{15}	1×10^{17}	1×10^{18}	1×10^{19}
Shallow uniform acceptor density, N_u (cm^{-3})	1×10^{16}	2×10^{14}	0	1×10^{1}	0	0	0
Defect type	-	Donor	Acceptor	Acceptor	Acceptor	-	-
Defect density (cm^{-3})	-	1×10^{13}	6×10^{15}	6×10^{16}	6×10^{16}	-	-

3. Results and Discussions

The proposed thin-film solar cell structure has been simulated by SCAPS-1D software. The schematic energy band diagram of this proposed structure with possible optical transitions have been demonstrated in **Figure 2**. Three novel buffer layer materials with different optical and electrical properties have been considered in this study. During illumination, the incident photons having energy larger than band gap energy of buffer layer material are possibly absorbed within the layer, while medium and lower energy or longer wavelength photons are mostly absorbed within the depletion region and within the p-CZTS absorber layer, respectively. For example, the photon having energy larger than 2.4 eV can be absorbed in the n-CdS based buffer layer for carriers generation. Intrinsic-ZnO acts as depletion region of charge carrier that has been used for the additional charge carriers generation by the solar energy.

Through these ways, incident solar energy generates electron-hole pairs in solar cell. The electron drifts towards the n- side buffer layer and makes the region negative. Similarly, hole drifts towards p side absorber layer and thereby makes this side positive. Since the electrons have a higher mobility and lifetime than holes, so the diffusion length of electron is kept larger than that of hole. This phenomenon has been assured in the structure by taking the thickness of absorber larger than that of buffer layer. This confirms the greater possibility of carrier collection across the load terminals. Thus, the effects of thicknesses of absorber layer as well as buffer layer on the performance parameters have been evaluated for the proposed structure. The uppermost n-ITO based ETL layer in this structure creates a potential barrier (ΔE_{v1}) to block hole flow while permits electron to be transported towards the front electrode. Similarly, the bottom

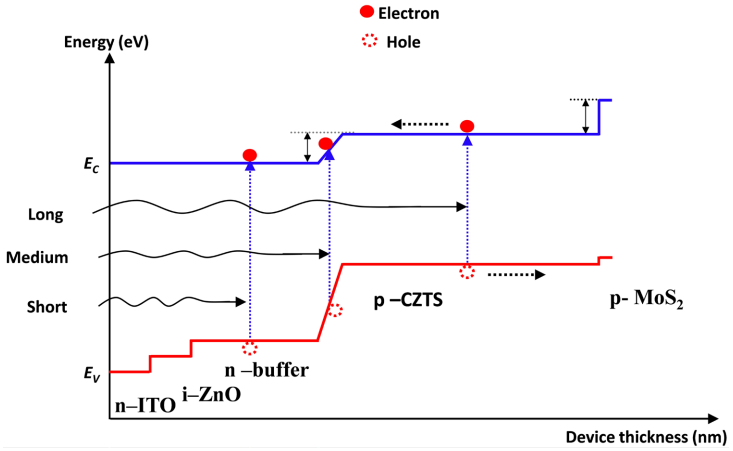

Figure 2. Schematic energy band diagram of the proposed thin-film solar cell structure, n-ITO/i-ZnO/n-buffer (CdS or ZnS or $Cd_{0.4}Zn_{0.6}S$)/p-CZTS/p-$MoSe_2$ with possible optical transitions.

most p-MoS_2 based HTL layer creates a potential barrier (ΔE_{C2}) to block electron flow while permits holes to be transported towards back electrode. Thus, the maximum number of electron-hole pair generation may possibly occur by the solar irradiation in the proposed thin-film solar cell structure. In addition, the losses of photo-generated electrons and holes are minimized by using appropriate HTL and ETL layers, respectively in the proposed structure.

3.1. Optimization of V_{oc}, J_{sc}, FF and η for the Various Thickness of CZTS Absorber Layer of Thin-Film Solar Cell

The thickness of the absorber layer is one of the most important parameters for increasing the performance of solar cells [33]. In this section, we firstly study the effect of absorber layer thickness of the proposed structure for achieving optimized V_{oc}, J_{sc}, FF and η. To demonstrate this, the performance characteristics of the thin film solar cell have been visualized as a function of thickness of absorber layer CZTS with three buffer layer materials as shown in **Figure 3**. For each simulation, the thickness of CZTS was varied from 100 to 2000 nm with a fixed buffer layer thickness of 50 nm at a temperature of 300 K. A single donor-type defect with a defect density of $1 \times 10^{13}\text{cm}^{-3}$ was introduced in the CZTS layer. By investigating the curves of J_{sc}, V_{oc}, FF and η as a function thickness of absorber layer as shown in **Figure 3(a)-(d)** respectively, it has been found that all performance parameters except V_{oc} showed similar changing tendency with changing absorber layer thickness in our study. The open circuit voltage shows a different approach.

As can be seen from the **Figure 3(b)**, **Figure 3(d)** and **Figure 3(a)**, performance parameters J_{sc}, FF and η upsurges linearly with rising thickness of CZTS absorber layer in the lower range from nearly 100 to 900 nm while V_{oc} is found to be saturated shown in **Figure 3(c)**. The results can be clarified by the facts that as the thickness of absorber layer increases, the photons absorption of incident light in this region becomes more which leads to excess electron-hole

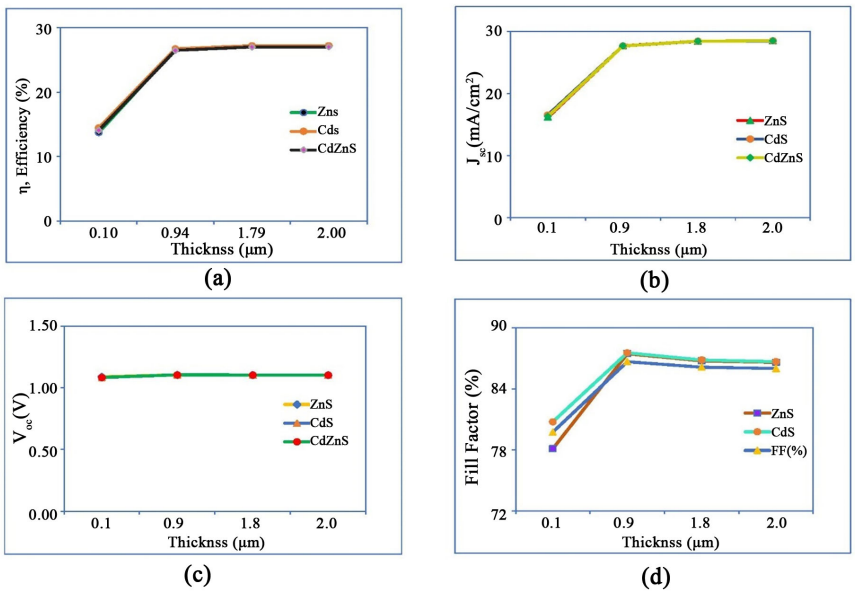

Figure 3. Dependency of V_{oc}, J_{sc}, FF and η parameters on the thickness of CZTS absorber layer of thin-film solar cell.

pair generation, and consequently promotes the short circuit current density in **Figure 3(b)**. The behavior of the FF is likely similar to that of V_{oc} and J_{sc} [34] while that of the efficiency can be illustrated by the behavior of V_{oc}, J_{sc} and FF [35]. Owing to the high-absorption coefficient of CZTS [15], a few hundred nanometer film is capable of absorbing enough sunlight. Therefore, the increment in J_{sc}, FF and η is found more significant at the thickness increment in the lower range from 100 nm to 900 nm of the absorber layer. In addition to the improvement of light absorption, the chance of carrier recombination also increases simultaneously with increasing thickness of absorber layer because the charge carriers have to travel longer distances for diffusion in a thicker absorber layer. Therefore, the rise in thickness above 900 nm leads the nearly saturated photo current density, fill-factor and efficiency. On the other hand, the open circuit voltage remained approximately constant since the increasing thickness of absorber layer results in the increment of carrier diffusion length, the probability of recombination rate of photo-generated carrier and life-time of photo-generated carrier have been affected, the amount of carrier collection at the electrodes decreases and consequently saturation in V_{oc} with increasing thickness. They all increase up to 900 nm and then possesses a slow increase in the efficiency up to almost 1800 nm and then shows a stiff straight line up to 2000 nm with really less comparable efficiency for all three materials.

In addition to the results, the numerical values of V_{oc}, J_{sc}, FF and η are comparable for the three buffer layer materials. For examples, the best efficiencies for ZnS/CZTS, CdS/CZTS, and $Cd_{0.4}Zn_{06}S$/CZTS structures were found as 26.71% at 0.9 μm, 26.72% at 1.3 μm, and 27.00% at 1.7 μm, respectively as can be seen from **Figure 3(a)**. As can be seen from **Table 1**, the highest electron mobility of $Cd_{0.4}Zn_{06}S$ among the three materials would result the highest pho-

to-voltaic conversion efficiency of the solar cell. For CdS, ZnS, and $Cd_{0.4}Zn_{06}S$ buffer layers, the upper limit of the CZTS absorber layer thickness was discovered at 900 nm, 1300 nm, and 1700 nm, respectively. With the $Cd_{04}Zn_{0\,6}S$ buffer layer, the greatest efficiency (27.0%) was discovered for the 1700 nm thick CZTS layer. Therefore, we have chosen the optimal thickness of CZTS absorber layer as around 2000 nm for further simulation because of optimized values of performances parameters.

3.2. Optimization of V_{oc}, J_{sc}, *FF* and η for the Various Thickness of Buffer Layer of Thin-Film Solar Cell

In this section, the buffer layer thickness was varied from 50 to 150 nm with a fixed absorber layer thickness of 2000 nm for simulation. A single acceptor-type defect with defect density of 6×10^{16} cm^{-3} was introduced in the buffer layer. **Figure 4** shows the variation of solar cell parameters as a function of buffer layer thickness.

It was noticeably found that all fundamentals parameters of solar cell remain same in their respective scales and independent of thickness of buffer layer in the relatively lower range for the three buffer layer materials. It is observed from **Figure 4(c)** that no significant variation on V_{oc} was found with increasing thickness of buffer layer for all buffer layer materials used in this study. This result has a good agreement with the previous reported result [36] [37]. As can be seen from **Figure 4(b)**, the short circuit density shows slightly degradation tendency with increasing of buffer layer thickness throughout the whole range for CdS and $Cd_{04}Zn_{06}S$. It finally becomes lowest at 150 nm. However, the parameter J_{sc} remains nearly independent of buffer layer thickness in case of ZnS material. Thus, although J_{sc} for three buffer layer materials possess approximately

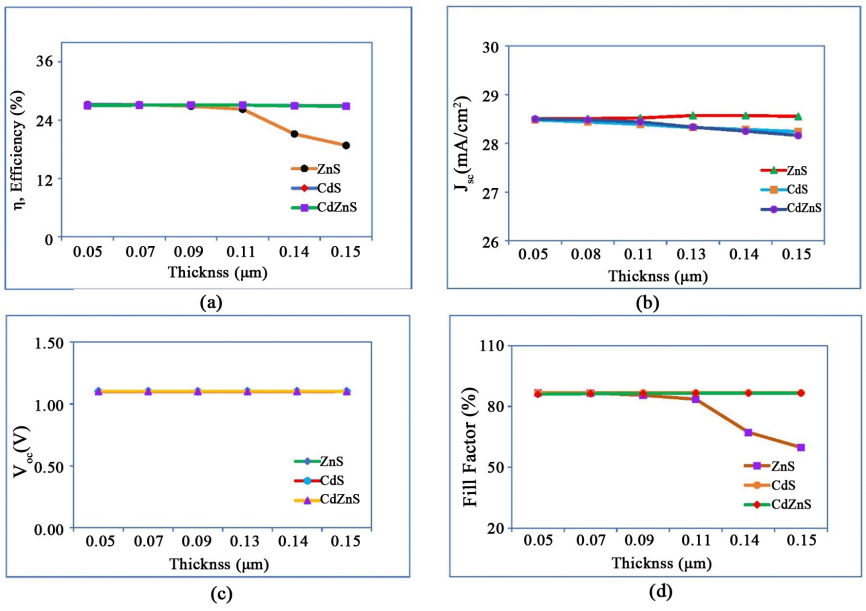

Figure 4. η, J_{sc}, V_{oc} and *FF* of thin-film solar cell as a function of thickness of buffer layer.

same value at lower thickness of buffer layer, it is possible to obtain higher short circuit density even at higher thickness of buffer layer, such as 150 nm by using ZnS instead of CdS and $Cd_{04}Zn_{06}S$ as buffer layer material. These obtained results can be explained by the facts that as the thickness of buffer layer increases, the diffusion length of carriers exceeds, this may lead to the inefficient photo-generated carrier's separation and collection, thereby may cause reduction in short circuit density [38]. Since the donor density of ZnS is much higher and uniformly distributed than that of CdS and $Cd_{04}Zn_{06}S$ as seen from **Table 1**, the reduction in J_{sc} was occurred less or negligible in ZnS than either CdS or $Cd_{04}Zn_{06}S$ at higher thickness. The fill factor for CdS and $Cd_{0.4}Zn_{0.6}S$ do not show any change with increasing buffer layer thickness. It has also been investigated that although FF and η seen from **Figure 4(d)** and **Figure 4(a)** respectively remained unchanged with increasing buffer layer thickness in the lower range from 50 nm to about 90 nm for ZnS buffer layer like CdS and $Cd_{04}Zn_{06}S$, after 90 nm thickness of buffer layer, both parameters of the solar cell for ZnS based buffer layer start decreasing dramatically. The decreasing behavior in FF for ZnS has been seen from around 65 nm which becomes more significant at 150 nm while η falls to almost 15% at 150 nm thickness, which is dissimilar to CdS and $Cd_{0\cdot4}Zn_{06}S$. Since CB effective density of states of ZnS is lower than that of CdS and $Cd_{04}Zn_{06}S$, thereby carrier concentrations and energy distributions of carriers are relatively lower. In addition, as the increasing buffer layer thickness results in longer diffusion length, higher series resistance and consequently increases the probability of carrier recombination rate. By these ways, the carriers separation becomes limited more in ZnS based buffer layer due to those facts at higher thickness of buffer layer [39] and thereby reduction in FF and finally fall in η as well. The obtained optimum efficiencies for CdS, ZnS, and $Cd_{04}Zn_{06}S$ buffers are 27.21%, 27.11%, and 27.11%, respectively which is shown in **Figure 4(a)**. Since band gap energy of ZnS is the highest than either CdS or $Cd_{0.4}Zn_{0.6}S$ as shown in **Table 1**, free electron is only generated by solar radiation having photon energy equal or greater than 3.5 eV. On the other hand, photon energy lower than 3.5 eV can also contribute to generate free electron in either CdS or $Cd_{0.4}Zn_{0.6}S$-based buffer layer since band gap energy of either CdS or $Cd_{0.4}Zn_{0.6}S$ is lower than 3.5 eV. This is one of the possible reasons for lowering the performance efficiency of ZnS based solar cell. From this study, we clarify that either CdS or $Cd_{0.4}Zn_{0.6}S$ is suitable as a buffer layer materials for any thickness of that layer in the range of 50-150 nm while the range is limited to 50-75 nm for ZnS.

3.3. Optimization of V_{oc}, J_{sc}, FF and η for the Various Doping Concentration of Absorber Layer Material of Thin-Film Solar Cell

The doping concentration of the absorber layer plays a significant role on the performance of solar cells. In this section, the doping concentration of the absorber layer material of the proposed structure has been evaluated for achieving

optimized V_{oc}, J_{sc}, FF and η for three buffer layer materials. To demonstrate this, the performance characteristics have been visualized as a function of doping concentration ranging from 1.00 E + 14 cm^{-1} to 1.00 E + 18 cm^{-1} of the absorber layer material CZTS with three buffer layer materials as shown in **Figure 5**. It is clearly found that all fundamentals parameters of solar cell remain almost constant with increasing acceptor doping concentration up to 1.00 E + 18 cm^{-1} for the two buffer layer materials ZnS and CdS. Solar cell with $Cd_{04}Zn_{06}S$ based buffer layer showed distinct behaviors in J_{sc}, FF η in the lower range of doping concentration of absorber layer which made it apart from ZnS and CdS. ZnS and CdS show almost stable J_{sc} values while J_{sc} of $Cd_{0.4}Zn_{0.6}S$ tends to decrease as the doping concentration is increased from 1.0 E + 14 cm^{-1} to 3.33 E + 17 cm^{-1} as shown in **Figure 5(b)**. After 3.33 E + 17 cm^{-1}, J_{sc} of $Cd_{0.4}Zn_{0.6}S$ becomes saturated. Since the electron mobility of $Cd_{0.4}Zn_{0.6}S$ is relatively higher than that of ZnS and CdS, it is apparent that the reduction in the width of depletion layer becomes sufficient while doping concentration increases in absorber layer with fixed thickness, thus much more photo-generated carriers rapidly recombine with holes, there is a weaken the carrier collection and finally reduction tendency in J_{sc} [40]. As the acceptor carrier concentration increases, open circuit voltage V_{oc} for all the buffer layer materials tend to maintain an almost stable voltage of 1.10 V which can be seen from **Figure 5(c)**. This can be explained by the facts that with increasing doping concentration at a constant thickness of absorber layer, the carrier collection probability becomes immediately saturated for the fixed collection length, thus additional charge carriers vanish by the recombination. This explanation has good agreement with previous report [41].

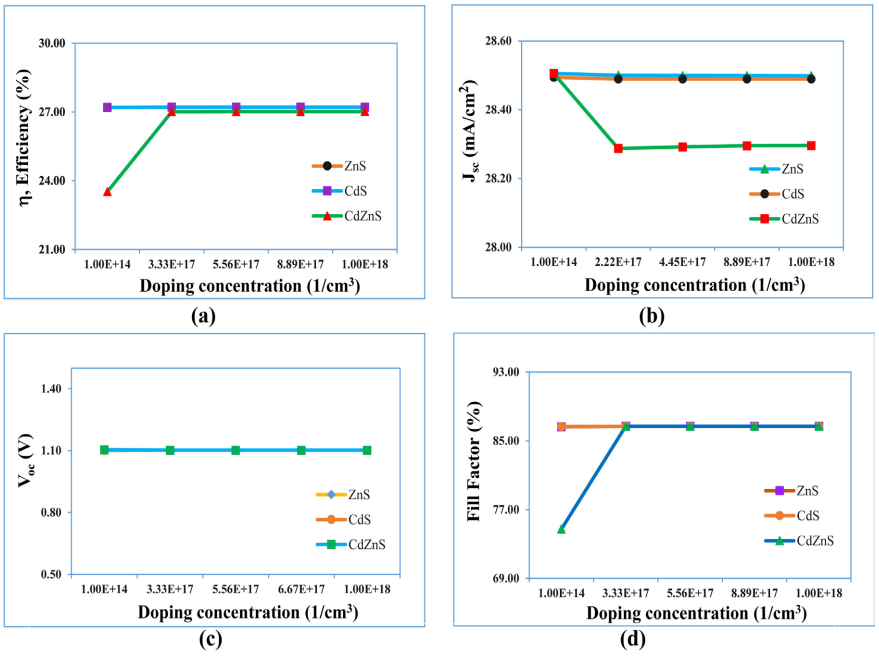

Figure 5. V_{oc}, J_{sc}, FF and η of thin-film solar cell as a function of doping concentration of the absorber layer material, CZTS with three buffer layer materials.

As can be seen from Figure 5(d), the FF of $Cd_{0.4}Zn_{0.6}S$ based solar cell increases linearly from very low value with increasing doping concentration from 1.00 E + 14 cm^{-1} to 3.33 E + 17 cm^{-1}, then stays a constant value till the last. However, ZnS and Cds shows almost constant of FF around 87% throughout the variation in doping concentration shown in Figure 5(d). The behavior of the η could be described by the whole behavior of the V_{oc}, J_{sc} and FF [35]. Similar shape like FF was found in η as shown in Fig. 5(a) for all buffer layer materials. ZnS and Cds shows almost constant of η around 27% throughout the variation in doping concentration while $Cd_{0.4}Zn_{0.6}S$ shows a uprising state in η from 1.00 E + 14 cm^{-1} but after 3.33 E + 17 cm^{-1}, it becomes a stable value of about 25% from up to 1.00 E + 18 cm^{-1}.

3.4. Evaluation of Temperature Effects on V_{oc}, J_{sc}, FF and η of Thin-Film Solar Cell

Operating temperature has a vital impact on the solar cells performances [42]. All of the simulations in this study were run at 300 K, which is the national average for ambient temperature. In this section, the temperature was raised from 290 K to 350 K to account for how the temperature affects V_{oc}, J_{sc}, FF and η of CZTS based thin-film solar cells for three buffer layer materials as demonstrated in Figure 6. It should be noted that the specified range of temperature considered in this section is consistence with the range of temperature subsists from winter to summer seasons in Bangladesh. It can be seen from the Fig. 6 that all parameters except short circuit current density have been strongly affected by the change in temperature in our study. It is seen from Figure 6(b) that the value of J_{sc} is found nearly temperature independent but strongly dependent and shows three

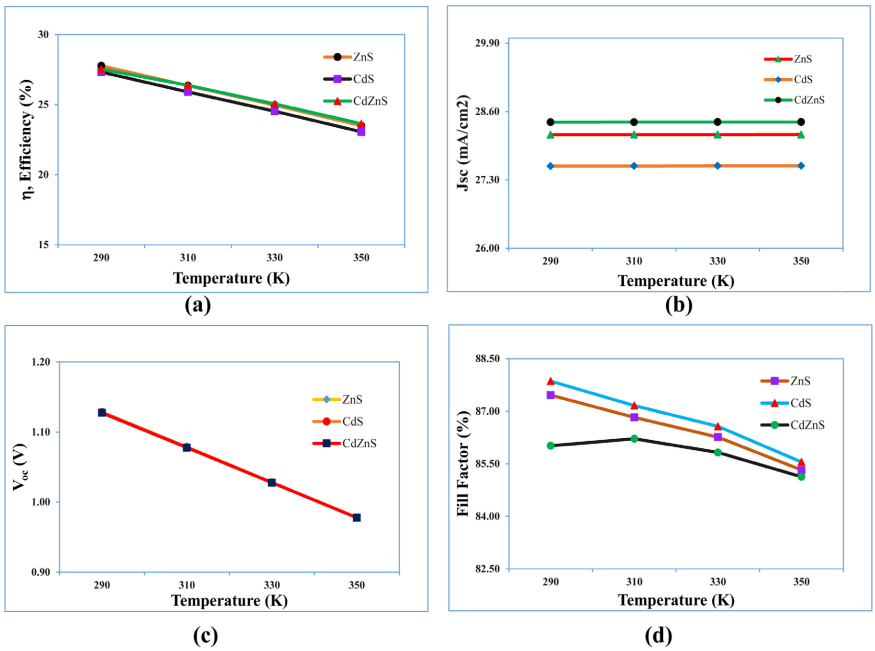

Figure 6. Temperature effects on V_{oc}, J_{sc}, FF and η of CZTS based thin-film solar cell for three buffer layer materials CdS, ZnS and $Cd_{0.4}Zn_{0.6}S$.

different straight lines for three different buffer layers. The value of J_{sc} can be restricted by the device ohmic losses such as series and shunt resistances, metal contact and recombination losses. The constant current density with increasing temperature apparently indicates that the combined effects of these mentioned parameters might mitigate the variation in J_{sc} in our simulation. The J_{sc} of $Cd_{0.4}Zn_{0.6}S$ is the highest, CdS shows the lowest. ZnS being in the middle of them.

It has been noticed that V_{oc}, FF and η in Figure 6(c), Figure 6(d) and Figure 6(a) respectively showed degradation tendency with increasing temperature from 290 K to 350 K for three novel buffer layer materials. The reasons of such degradation can be explained by the facts that temperature affects solar cell performance negatively through touching several parameters of materials simultaneously. Increasing temperature shifts the band gap energy of the semiconductors to lower energy[43] and also simultaneously increases the velocity-instability of charged particles [44], reverse saturation current and resistivity of the materials as well. As a result, the probability of recombination rate of charge carriers before reaching the depletion region promotes and eventually degradation of V_{oc} occurs as seen from Figure 6(c). Furthermore, the behavior of FF is dependent on the combined behavior of V_{oc} and J_{sc} [45] [46]. Constant J_{sc} while decrement in V_{oc} jointly led to a decrease in FF of the device for all buffer layer materials. It is found from Figure 6(d) that the FF of ZnS and CdS shows decreasing in parallel line, while CdS showing the higher between the two. $Cd_{04}Zn_{06}S$ shows little different approach than the other two materials during temperature uprising in the lower range. It slightly increases first from 290 K to 310 K, then starts to decrease gradually like to either ZnS or CdS. The value of η reflects the total behavior of V_{oc}, J_{sc} and FF. Constant J_{sc} and decrement in both V_{oc} and FF showed the way to a decrease in the η of the device as shown in Figure 6(a). From the simulation, the best efficiencies for CdS/CZTS, ZnS/CZTS, and $Cd_{0.4}Zn_{0.6}S$/CZTS were found as 27.33%, 27.78%, and 27.54%, respectively, at a temperature of 290 K. In addition, it was also noticeably that $Cd_{04}Zn_{06}S$ offers the most efficient short circuit current density while least FF in this section.

3.5. Comparison among Various Photovoltaic Parameters of the Proposed Model with the Related Thin-Film Solar Cell Models Reported Previously

Finally, we have tried to make comparison between our proposed model and the related models of the other researchers reported previously in terms of performance parameters as shown in Table 2.

Our proposed model of thin-film solar cell supports comparatively higher open circuit voltage, short-circuited current density, fill-factor and efficiency successfully with lower toxicity.

Table 2. Comparison among photovoltaic parameters of the solar cell based on CZTS absorber layer.

Thin-film solar cell structure	$V_{oc}(V)$	$J_{sc}\left(\frac{mA}{cm^2}\right)$	***FF*** **(%)**	$\eta(\%)$	Reference
MoS_2/CZTS/CdZnS/ZnO/ITO	~1.10	~27.00	~87.0	~27.0	proposed
MoS_2/CZTS/CdS/ZnO	0.7159	24.9857	66.58	11.91	
MoS_2/CZTS/SnS2/ZnO	0.7178	26.9976	65.67	12.73	[47]
MoS_2/CZTS/ZTO/ZnO	0.7157	24.9324	66.62	11.89	
FTO/ZnO/CdS/CZTS/Mo	0.4400	25.5600	75.93	8.38	
FTO/ZnO/CdS/CZTS/Mo	0.4722	23.3868	77.44	8.55	[39]
FTO/ZnO/CdS/CZTS/CZTSe/Mo	0.9355	28.2630	83.31	22.03	

4. Conclusion

The ecofriendly CZTS based thin-film solar cell structure with three novel buffer layer materials have been studied and simulated by using Solar Cell Capacitance Simulator in one dimensional (*SCAPS-1D*) software program. The effects of thickness of absorber layer and buffer layer, doping concentration of absorber layer material as well as operating temperature on the solar cell performance have been considered in this study. The four fundamental performance parameters V_{oc}, J_{sc}, FF and η of this structure have been investigated and optimized. The investigation of performance parameters for various thicknesses of CZTS absorber layer has clarified that the thickness around 2000 nm is preferable for achieving better efficiency from the proposed solar cell. Although the efficiency of $Cd_{0.4}Zn_{0.6}S$, ZnS and CdS are nearly comparable, $Cd_{0.4}Zn_{0.6}S$ is preferable to use as buffer layer for its non-toxic property. In addition, the evaluation of performance as a function of buffer layer thickness for $Cd_{0.4}Zn_{0.6}S$, ZnS and CdS exposed that the optimum buffer layer thickness for $Cd_{0.4}Zn_{0.6}S$ was in the range from 50 to 150 nm while ZnS offered only 50–75 nm. Furthermore, it has been explored by evaluating the dependence of V_{oc}, J_{sc}, FF and η on doping concentration of absorber layer materials with three buffer materials that dramatic behavior was found in all performance parameter for the $Cd_{0.4}Zn_{0.6}S$ based buffer layer with doping concentration of absorber layer. Finally, the studied of the efficiency and other performance parameters on temperature ranging from 290 K to 350 K have been exposed that 290 K is the suitable working temperature of solar cell for stable operation. This research finding would be very helpful for developing nanotechnology based solar energy technology for reducing global energy crisis as well as green-house gas emission simultaneously and sustainably in the world.

Acknowledgement

We are grateful to the Department of Electrical and Electronic Engineering, Hajee Mohammad Danesh Science and Technology University, Dinajpur-5200, Bangladesh for providing necessary technical supports.

Funding

The research works have been conducted by self-funded.

Data Availability

The data of this study are available from the corresponding author upon reasonable request.

Conflicts of Interest

The authors declare no conflicts of interest regarding the publication of this paper.

References

[1] Owusu, P.A. and Asumadu-Sarkodie, S. (2016) A Review of Renewable Energy Sources, Sustainability Issues and Climate Change Mitigation. *Cogent Engineering*, **3**, Article ID: 1167990. https://doi.org/10.1080/23311916.2016.1167990

[2] Shiyani, T., Mahapatra, S.K. and Banerjee, I. (2023) Plasmonic Solar Cells. In: Inamuddin, Ahamed, M.I., Boddula, R. and Rezakazemi, M., Eds., *Fundamentals of Solar Cell Design*, John Wiley & Sons, Hoboken, 55-81. https://doi.org/10.1002/9781119725022.ch2

[3] Bilgen, S. (2014) Structure and Environmental Impact of Global Energy Consumption. *Renewable and Sustainable Energy Reviews*, **38**, 890-902. https://doi.org/10.1016/j.rser.2014.07.004

[4] Islam, M.M. and Hasanuzzaman, M. (2020) Introduction to Energy and Sustainable Development. In: Hasanuzzaman, M.D. and Rahim, N.A., Eds., *Energy for Sustainable Development*: *Demand*, *Supply*, *Conversion and Management*, Elsevier, Amsterdam, 1-18. https://doi.org/10.1016/B978-0-12-814645-3.00001-8

[5] Maka, A.O.M. and Alabid, J.M. (2022) Solar Energy Technology and Its Roles in Sustainable Development. *Clean Energy*, **6**, 476-483. https://doi.org/10.1093/ce/zkac023

[6] Kabir, E., Kumar, P., Kumar, S., Adelodun, A.A. and Kim, K.H. (2018) Solar Energy: Potential and Future Prospects. *Renewable and Sustainable Energy Reviews*, **82**, 894-900. https://doi.org/10.1016/j.rser.2017.09.094

[7] NREL (2021) Documenting a Decade of Cost Declines for PV Systems Documenting a Decade of Cost Declines for PV Systems. The National Renewable Energy Laboratory (NREL), Golden, 23-25. https://www.nrel.gov/news/program/2021/documenting-a-decade-of-cost-declines-for-pv-systems.html

[8] Yasodharan, R., Senthilkumar, A.P., Mohankumar, P. and Ajayan, J. (2020) Investigation and Influence of Layer Composition of Tandem Perovskite Solar Cells for Applications in Future Renewable and Sustainable Energy. *Optik* (*Stuttg*), **212**, Article ID: 164723. https://doi.org/10.1016/j.ijleo.2020.164723

[9] Mazzucato, S., *et al*. (2012) Dilute Nitride and GaAs N-I-P-I Solar Cells. *Nanoscale Research Letters*, **7**, Article No. 631. https://doi.org/10.1186/1556-276X-7-631

[10] Deshpande, R.A. (2021) Advances in Solar Cell Technology: An Overview. *Journal of Scientific Research*, **65**, 72-75. https://doi.org/10.37398/JSR.2021.650214

[11] Moon, S., Kim, K., Kim, Y., Heo, J. and Lee, J. (2016) Highly Efficient Single-Junction GaAs Thin-Film Solar Cell on Flexible Substrate. *Scientific Reports*, **6**, Article No. 30107. https://doi.org/10.1038/srep30107

[12] Elshorbagy, M.H., Abdel-Hady, K., Kamal, H. and Alda, J. (2017) Broadband Anti-Reflection Coating Using Dielectric Si_3N_4 Nanostructures. Application to Amor-

phous-Si-H Solar Cells. *Optics Communications*, **390**, 130-136. https://doi.org/10.1016/j.optcom.2016.12.062

[13] Ingrid Repins, Y., *et al*. (2008) 19.9%-Efficient ZnO/CdS/CuInGaSe$_2$ Solar Cell with 81.2% Fill Factor. *Progress in Photovoltaics*: *Research and Applications*, **16**, 235-239. https://doi.org/10.1002/pip.822

[14] Jackson, P., *et al*. (2011) New World Record Efficiency for Cu(In,Ga)Se$_2$ Thin-Film Solar Cells beyond 20%. *Progress in Photovoltaics*: *Research and Applications*, **19**, 894-897. https://doi.org/10.1002/pip.1078

[15] Swati, S., Matin, R., Bashar, S. and Mahmood, Z. (2018) Experimental Study of the Optical Properties of Cu_2ZnSnS_4 Thin Film Absorber Layer for Solar Cell Application. *Journal of Physics*: *Conference Series*, **1086**, Article ID: 012010. https://doi.org/10.1088/1742-6596/1086/1/012010

[16] Wang, H. and Gong, Y. (2011) Low Temperature Synthesized Quaternary Chalcogenide Cu_2ZnSnS_4 from Nano-Crystallite Binary Sulfides. *Journal of the Electrochemical Society*, **15**, H800-H803. https://doi.org/10.1149/1.3598168

[17] Ahmoum, M., Chelvanathan, H. and Su'Ait, P. (2021) Sol-Gel Prepared Cu_2ZnSnS_4 (CZTS) Semiconductor Thin Films: Role of Solvent Removal Processing Temperature. *Materials Science in Semiconductor Processing*, **132**, Article ID: 105874. https://doi.org/10.1016/j.mssp.2021.105874

[18] Mkawi, E.M., Al-Hadeethi, Y., Shalaan, E. and Bekyarova, E. (2020) Solution-Processed Sphere-Like Cu_2ZnSnS_4 Nanoparticles for Solar Cells: Effect of Oleylamine Concentration on Properties. *Applied Physics A*: *Materials Science and Processing*, **126**, Article No. 50. https://doi.org/10.1007/s00339-019-3233-1

[19] Yu, S.M., Lim, K.S., Shin, D.W., Oh, T.S. and Yoo, J.B. (2017) Effect of the Intermediate Sulfide Layer on the Cu_2ZnSnS_4-Based Solar Cells. *Journal of Materials Science*: *Materials in Electronics*, **28**, 5696-5702. https://doi.org/10.1007/s10854-016-6241-3

[20] Eisele, W., *et al*. (2003) XPS, TEM and NRA Investigations of Zn(Se,OH)/Zn(OH)$_2$ Films on Cu(In,Ga)(S,Se)$_2$ Substrates for Highly Efficient Solar Cells. *Solar Energy Materials and Solar Cells*, **75**, 17-26. https://doi.org/10.1016/S0927-0248(02)00104-6

[21] Yasin, S., Waar, Z.A. and Al Zoubi, T. (2020) Development of High Efficiency CZTS Solar Cell through Buffer Layer Parameters Optimization Using SCAPS-1D. *Materials Today*: *Proceedings*, **33**, 1825-1829. https://doi.org/10.1016/j.matpr.2020.05.064

[22] Akcay, S., Zaretskaya, N. and Ozcelik, E. (2019) Development of a CZTS Solar Cell with CdS Buffer Layer Deposited by RF Magnetron Sputtering. *Journal of Alloys and Compounds*, **772**, 782-792. https://doi.org/10.1016/j.jallcom.2018.09.126

[23] Nguyen, M., *et al*. (2015) ZnS Buffer Layer for $Cu_2ZnSn(SSe)_4$ Monograin Layer Solar Cell. *Solar Energy*, **111**, 344-349. https://doi.org/10.1016/j.solener.2014.11.006

[24] Mazumder, S. and Senthilkumar, K. (2022) Device Study and Optimisation of CZTS/ZnS Based Solar Cell with CuI Hole Transport Layer for Different Conduction Band Offset. *Solar Energy*, **237**, 414-431. https://doi.org/10.1016/j.solener.2022.03.036

[25] Zhou, Z., Zhao, K. and Huang, F. (2010) Optical Properties of $Cd_{1-x}Zn_xS$ Thin Films for CuInGaSe$_2$ Solar Cell Application. *Materials Research Bulletin*, **45**, 1537-1540. https://doi.org/10.1016/j.materresbull.2010.06.005

[26] Zhang, X., *et al*. (2022) Synthesis of CdZnS Buffer Layer and Its Impact on $Cu_2ZnSn(S,Se)_4$ Thin Film Solar Cells. *Journal of Materials Science*: *Materials in*

Electronics, **33**, 2399-2405. https://doi.org/10.1007/s10854-021-07446-5

[27] Zein, W., Alanazi, T.I., Salah, M.M. and Saeed, A. (2023) Concurrent Design of Alloy Compositions of CZTSSe and CdZnS Using SCAPS Simulation: Potential Routes to Overcoming VOC Deficit. *Energies*, **16**, Article No. 5754. https://doi.org/10.3390/en16155754

[28] Jhuma, F.A., Shaily, M.Z. and Rashid, M.J. (2019) Towards High-Efficiency CZTS Solar Cell through Buffer Layer Optimization. *Materials for Renewable and Sustainable Energy*, **8**, Article No. 6. https://doi.org/10.1007/s40243-019-0144-1

[29] Verschraegen, M. and Burgelman, J. (2007) Numerical Modeling of Intra-Band Tunneling for Heterojunction Solar Cells in Scaps. *Thin Solid Films*, **515**, Article No. 6276. https://doi.org/10.1016/j.tsf.2006.12.049

[30] Hima, N. and Lakhdar, A. (2020) Enhancement of Efficiency and Stability of $CH_3NH_3GeI_3$ Solar Cells with $CuSbS_2$. *Optical Materials* (*Amst*), **99**, Article ID: 109607. https://doi.org/10.1016/j.optmat.2019.109607

[31] Pindolia, G., Shinde, S.M. and Jha, P.K. (2022) Optimization of an Inorganic Lead Free $RbGeI_3$ Based Perovskite Solar Cell by SCAPS-1D Simulation Optimization of an Inorganic Lead Free $RbGeI_3$ Based Perovskite Solar Cell by SCAPS-1D Simulation. *Solar Energy*, **236**, 802-821. https://doi.org/10.1016/j.solener.2022.03.053

[32] Yasin, S., Waar, Z.A. and Al Zoubi, T. (2020) Development of High Efficiency CZTS Solar Cell through Buffer Layer Parameters Optimization Using SCAPS-1D. *Materials Today*: *Proceedings*, **33**, 1825-1829. https://doi.org/10.1016/j.matpr.2020.05.064

[33] Ouslimane, T., Et-Taya, L., Elmaimouni, L. and Benami, A. (2021) Impact of Absorber Layer Thickness, Defect Density, and Operating Temperature on the Performance of $MAPbI_3$ Solar Cells Based on ZnO Electron Transporting Material. *Heliyon*, **7**, E06379. https://doi.org/10.1016/j.heliyon.2021.e06379

[34] Mbopda Tcheum, J.M.B., Teyou Ngoupo, G.L., Ouédraogo, A., Guirdjebaye, S. and Ndjaka, N. (2020) Numerical Analysis of Ultrathin Cu(In,Ga)Se_2 Solar Cells with Zn(O,S) Buffer Layer. *Pramana*, **94**, Article No. 111. https://doi.org/10.1007/s12043-020-01977-y

[35] Baloch, A.A.B., Aly, S.P., Hossain, M.I. and El-Mellouhi, F. (2017) Full Space Device Optimization for Solar Cells. *Scientific Reports*, **7**, Article No. 11984. https://doi.org/10.1038/s41598-017-12158-0

[36] Chang, K., Tian, W.H., Fang, H.M., Guo, G.C., Wang, D. and Zhao, Z. (2019) Simulation of Innovative High Efficiency Perovskite Solar Cell with Bi-HTL: NiO and Si Thin Films. *Solar Energy*, **186**, 323-327. https://doi.org/10.1016/j.solener.2019.05.017

[37] Garmim, T., *et al*. (2022) Effect of Alternative Buffer Layers for SnS Based Solar Cells: Numerical Analysis Using SCAPS-1D. *Materials Today*: *Proceedings*, **66**, 146-150. https://doi.org/10.1016/j.matpr.2022.04.289

[38] Wang, Y., *et al*. (2015) Towards Printed Perovskite Solar Cells with Cuprous Oxide Hole Trans-Porting Layers: A Theoretical Design. *Semiconductor Science and Technology*, **30**, Article ID: 054004. https://doi.org/10.1088/0268-1242/30/5/054004

[39] Belarbi, F., Rahal, W., Rached, D., Benghabrit, S. and Adnane, M. (2020) A Comparative Study of Different Buffer Layers for CZTS Solar Cell Using Scaps-1D Simulation Program. *Optik* (*Stuttg*), **216**, Article ID: 164743. https://doi.org/10.1016/j.ijleo.2020.164743

[40] Zhou, X. and Han, J. (2020) Design and Simulation of C_2N Based Solar Cell by

SCAPS-1D Software. *Materials Research Express*, **7**, Article ID: 126303. https://doi.org/10.1088/2053-1591/abcdd6

[41] Moustafa, M., Al Zoubi, T. and Yasin, S. (2022) Exploration of CZTS-Based Solar Using the ZrS_2 as a Novel Buffer Layer by SCAPS Simulation. *Optical Materials* (*Amst*), **124**, Article ID: 112001. https://doi.org/10.1016/j.optmat.2022.112001

[42] Daoudia, A.K., El Hassouani, Y. and Benami, A. (2016) Investigation of the Effect of Thickness, Band Gap and Temperature on the Efficiency of CIGS Solar Cells through SCAPS-1D. *International Journal of Engineering and Technology Research*, **6**, 71-75.

[43] Varshni, Y.P. (1967) Temperature Dependence of the Energy Gap in Semiconductors. *Physica*, **34**, 149-154. https://doi.org/10.1016/0031-8914(67)90062-6

[44] Alam, I. and Ashraf, A. (2020) Effect of Different Device Parameters on Tin Based Perovskite Solar Cell Coupled with In_2S_3 Electron Transport Layer and CuSCN and Spiro-OMeTAD Alternative Hole Transport Layers for High Efficiency Performance. *Energy Sources*, *Part A*: *Recovery*, *Utilization*, *and Environmental Effects*, **159**, 1-17. https://doi.org/10.1080/15567036.2020.1820628

[45] Priyanka Singh, N.M.R. (2012) Temperature. *Solar Energy Materials and Solar Cells*, **101**, 36-45. https://doi.org/10.1016/j.solmat.2012.02.019

[46] Abdelfatah, M., *et al.* (2016) Solar Energy Materials and Solar Cells Fabrication and Characterization of Low Cost Cu_2O/ZnO: Al Solar Cells for Sustainable Photovoltaics with Earth Abundant Materials. *Solar Energy Materials and Solar Cells*, **145**, 454-461. https://doi.org/10.1016/j.solmat.2015.11.015

[47] Moon, M.M.A., Ali, M.H., Rahman, M.F. and Hossain, J. (2020) Design and Simulation of FeSi-Based Novel Heterojunction Solar Cells for Harnessing Visible and Near-Infrared Light. *Physica Status Solidi*, **217**, Article ID: 1900921. https://doi.org/10.1002/pssa.201900921